Polyamides Based on the Renewable Monomer, 1,13-Tridecane Diamine I: Synthesis and Characterization of Nylon 13,T.

Jie He,[1] Satyabrata Samanta,[1] Sermadurai Selvakumar,[2] Jessica Lattimer,[3] Chad Ulven,[3] Mukund Sibi,[2] James Bahr,[1] and Bret J. Chisholm[1,4]*

[1]*Center for Nanoscale Science and Engineering*
[2]*Department of Chemistry and Biochemistry*
[3]*Department of Mechanical Engineering*
[4]*Department of Coatings and Polymeric Materials*
North Dakota State University
Fargo, ND 58102

Abstract

Nylon 13,T was successfully synthesized and chemical composition, thermal properties, crystal structure, and moisture absorption characterized. Melting temperature and glass transition temperature were determined to be 263 °C and 90 °C, respectively, while the equilibrium melting temperature was determined to be 289 °C. Characterization of the crystallization kinetics showed that nylon 13,T exhibits very fast crystallization compared to the industrially important nylons, nylon 6 and nylon 6,6. In addition, the moisture absorption of nylon 13,T was dramatically lower than nylon 6 and nylon 6,6 which is consistent with the much lower amide content of nylon 13,T. The crystal structure was determined to be pseudohexagonal.

* To Whom Correspondence Should be Addressed: Bret.Chisholm@ndsu.edu

Keywords: Nylon; Polyamide; Semicrystalline; Crystallization Kinetics; Renewables

Introduction

Since fossil resources are finite, there is an ongoing need for the development of fuels and materials from renewable resources. With regard to the chemical industry, most all organic compounds are derived from fossil resources.[1] In the United States, approximately 13 percent of crude oil is used for the production of nonfuel chemicals.[2] The primary renewable feedstocks for the chemical industry include plant oils, polysaccharides, sugars, and wood. Of these, plant oils are particularly useful since they can be easily isolated and derivatized to produce a variety of useful chemicals.[3,4] Examples of crops that produce industrially significant volumes of oil include soybeans, sunflowers, oil palm, peanuts, coconuts, crambe, mustard, rapeseed, and safflower. The oils derived from these different crops consist predominantly of triglycerides. A triglyceride is the triester product of glycerol and three fatty acids. The fatty acid composition of the triglycerides vary based on the oil source. Fatty acids primarily vary with respect to the length of the hydrocarbon chain, the degree of unsaturation, and stereochemistry associated with the unsaturation. The utility of a given plant oil as chemical or material feedstock largely depends on the fatty acid composition. For example, coconut oil and palm kernel oil are particularly suited for the production of surfactants and cosmetics because they possess relatively high fractions of short and medium chain length (mainly 12 and 14 carbon atoms) fatty acids; while soybean and linseed oil are used in coating applications since they possess the relatively high levels of the unsaturation needed for crosslinking.

The unsaturation found in plant oil triglycerides has enabled their use as feedstocks for surface coatings, polymer foams, plastics, and rubber compounds.[5-7] For surface coatings, the unsaturation enables crosslinked networks to be produced via an oxidative coupling process referred to as auto-oxidation.[8] In addition, the double bonds have been derivatized to produce epoxy, hydroxy, and acrylate-functional derivatives useful for coating applications.[9] Besides coating applications, hydroxy-

functional plant oils have found utility in the production of polyurethane foams. For the production of plastics and additives for plastics, unsaturated fatty acids from plant oils have been oxidized to produce dicarboxylic acids useful for the production of polyesters and polyamides.[10-12] Plant oils that produce high contents of oleic acid are useful for the production of the nine carbon dicarboxylic acid, azelaic acid; while the ten carbon dicarboxylic acid, sebacic acid, can be obtained from castor oil by alkali pyrolysis of ricinoleic acid.[13,14] The thirteen carbon dicarboxylic acid, brassylic acid, can be derived from plant oils that contain significant levels of erucic acid esters, such as crambe and rapeseed oil.[15] Due to the long aliphatic chain associated with these plant oil-based dicarboxylic acids, the glass transition temperature (Tg) and melting temperature (Tm) of polyesters and polyamides produced using linear aliphatic diols and diamines, respectively, tend to be relatively low compared to commercially important polyesters and polyamides such as polyethylene terephthalate, polybutylene terephthalate, nylon 6, and nylon 6,6. Some examples of polyamides based on plant oil-derived dicarboxylic acids that have been studied include nylon 6,10,[16] nylon 4,10,[17] nylon 6,9,[18] and nylon 13,13.[19]

In order to increase thermal properties such as Tg and Tm while maintaining the use of a plant oil-based starting material, a plant oil-derived dicarboxylic acid can be converted to a diamine and subsequently polymerized with aromatic diacid monomers such as terephthalic acid (TA) and isophthalic acid. Introducing aromatic rings into a polyamide greatly increases the rigidity of the polymer backbone resulting in significant increases in Tg and Tm. Kuraray has commercialized polyamide copolymers based on 1,9-nonane diamine (NDA) and TA under the tradename Genestar™.[20,21] These NDA-based semi-aromatic polyamides possess Tms in the range of 290 °C.[22] Nylon 10,T which is the homopolymer of 1,10-decane diamine and TA, has been reported to possess a Tm of approximately 305 °C. Considering the exceptionally high Tms that can be achieved by polymerizing a plant oil-derived diamine with TA, it was of interest to investigate the properties of poly(tridecamethylene terephthalamide) (nylon 13,T). To the best of the author's knowledge, the properties of nylon 13,T have not been previously reported. Since 1,13-tridecane diamine (TDA) can be derived from erucic acid, nylon 13,T has a renewable content of 63 weight percent.

Experimental

Materials. All materials were used without further purification. Thionyl chloride and TA were purchased from Aldrich, while 1,13-tridecanedioic acid (i.e. brassylic acid) was obtained from TCI America. $LiAlH_4$ and dichloroacetic acid were obtained from Alfa Aesar. Tetrahydrofuran (99%), Dichloromethane (99.5%) were purchased from Alfa Aesar and anhydrous Na_2SO_4 (99%), NaOH (98%) were obtained from Aldrich.

Synthesis of TDA. 1,13-tridecanedioyl dichloride was synthesized according to the method described by Moreau et al[23]. To a solution of 1,13-tridecanedioic acid (2.44 g, 10 mmol) in dry methylene chloride (25 mL), thionyl chloride (36 mmol) was slowly added at room temperature and the mixture refluxed overnight. The methylene chloride and excess thionyl chloride were evaporated under vacuum and the liquid product purified by distillation. The yield of 1,13-tridecanedioyl dichloride was 75%

1,13-tridecanedioyl dichloride was converted to 1,13-tridecanediamide as follows: To a solution of 1,13-tridecanedioyl dichloride (2.81 g, 10 mmol) in dry tetrahydrofuran (50 mL), liquid ammonia was added dropwise at 0 ^{0}C over the period of 1 hour. The reaction mixture was then stirred at room temperature overnight. Volatiles were removed under vacuum, and the resulting solid (i.e. 1,13-tridecanediamide) was filtered and washed with water. The yield was approximately quantitative. ^{1}H NMR (400 MHz, DMSO-d6) δ 1.96 (m, 18H), 1.43 (m, 4H), 1.97 (t, J = 7.2 Hz, 4H), 6.6 (bs, 2H), 7.1 (bs, 2H).

From 1,13-tridecanediamide, TDA was produced as follows: To a suspension of $LiAlH_4$ (10 mmol) in THF (50 mL), 1,13-tridecanediamide (0.484 g, 2 mmol) was slowly added with stirring at 0 ^{0}C. After complete addition of 1,13-tridecanediamide, the mixture was heated and allowed to reflux for 12 hours. Next, the reaction mixture was cooled to room temperature and excess $LiAlH_4$ was quenched with a mixture of 4N aqueous NaOH (400 µL) and water (1.2 mL). The reaction mixture was filtered over celite and washed with THF. The filtrate was dried over anhydrous Na_2SO_4 and the solvent removed using a rotary evaporator to produce pure TDA as a white solid with a melting temperature of 95-98 ^{0}C. Yield: 72 %. ^{1}H NMR (400 MHz, CDCl3) δ 1.25 (m, 18H), 1.42 (m, 4H), 2.67 (t, J = 9.2 Hz, 4H).

Synthesis of the monomer salt of TA and TDA. The monomer salt of TA and TDA was produced as follows: 5.35 g (25 mmol) of TDA, 4.15 g (25 mmol) of TA, and 125 mL of 4/1 v/v ethanol/water were charged to a 250 ml round-bottom flask and the mixture stirred at 90 ^{0}C for two hours. During heating, initially insoluble material was dissolved. Next, the solution was cooled to room temperature and the volume reduced to 1/3 by stripping volatiles with a rotary evaporator. To this solution, 40 mL of hexane was added and the flask stored in a refrigerator overnight. The white crystalline solid produced was isolated by filtration, washed with ethanol (10 mL), and dried under vacuum. Yield: 7.75 g (82%). ^{1}H NMR (400 MHz, CD_3OD) δ 1.24 – 1.29 (m, 18 H); 1.59 – 1.63 (m, 4H); 2.88 (t, 7.8 Hz, 4H); 7.95 (s, 4H).

Synthesis of nylon 13,T. Nylon 13,T was synthesized using a two-step process. First, an oligomer/prepolymer was produced by dissolving 10 g of TA/TDA monomer salt in 40 g of hot deionized water that had been degassed by purging with nitrogen for 20 minutes. The solution was transferred to a stainless steel pressure vessel, degassed five times, and finally kept under vacuum. The reaction mixture was heated under magnetic stirring to 220 ^{0}C which produced a pressure of approximately 350 psi. After reaching 220 ^{0}C, the reaction mixture was held at this temperature for two hours. After this two hour period, the pressure was

released to remove the water, and the material held under vacuum for an additional 1.5 hours at 220 ^{0}C. The reactor was then allowed to cool to room temperature under vacuum before removing the prepolymer from the reactor. To produce high molecular weight polymer from the prepolymer, 3 to 10 g of the prepolymer was added to a glass tube equipped with an overhead mechanical strirrer, vacuum line, and nitrogen purge. After evacuating the air from the tube, it was placed in a 290 ^{0}C oil bath which melted the prepolymer. The molten polymer was stirred under high vacuum at 290 ^{0}C for 1.5 hours. After this period, the tube was allowed to cool to room temperature under vacuum. The cream-colored polymer was isolated by breaking the glass tube.

Characterization: Before characterization using thermal techniques, all polymer samples were dried in a vacuum oven at 100 °C overnight. Differential scanning calorimetry (DSC) experiments were performed using a TA Q2000 instrument. The experiments were conducted under a N_2 atmosphere, and the instrument was calibrated with an indium standard. Sample sizes ranged from 4.5-7.5 mg. For characterization of the melting transition, specimens were cooled from 300 °C to 0 °C at a cooling rate of 20 °C/min and then reheated to 300 °C at different heating rates (i.e. 5, 20, and 40 °C/min.). Isothermal crystallization kinetics were determined by cooling specimens from 300 °C to the predetermined crystallization temperature at a rate of 100 ˚C/minute and observing the heat flow as a function of time.

The thermal stability of nylon 13,T was characterized using a Q500 Thermogravimetric Analyzer from TA Instruments (New Castle, DE). Samples (8.5-10 mg) were heated from 25 °C to 1000 °C at a heating rate of 10 °C/min under a nitrogen or air atmosphere.

X-Ray Diffraction (XRD) data was collected in Bragg−Brentano geometry using a Rigaku Ultima IV instrument (Cu Kα radiation, voltage 40 kV, current 44 mA). The samples were scanned from 2-60 degrees 2-Theta with a step size of 0.025 degrees and a scan time of 10 sec/step. The samples were rotated at 25 rpm. Slits used were a 2/3 mm divergence slit, 10 mm height limiting slit, 5 degree soler slits, 2/3 mm scattering slit, and 0.3mm receiving slit.

The solution viscosity of the nylon 13,T sample produced for the study was determined using an Ubbelohde viscometer (model 1B) from Technical Glass Products Inc. (Dover, NJ). A 0.10 wt.% polymer solution in dichloracetic acid was prepared and passed through a 0.2 um Millipore filter. The intrinsic viscosity [η] of the polymer was measured at 25 $\pm$ 0.1 °C using the single-point viscosity equation described by Soloman and Cuita:[24]

$$[\eta]=\text{Sqrt}\ [2(\eta_{sp} - \ln \eta_{rel})]/c \qquad \text{(I)}$$

where η_{sp} and η_{rel} are the specific viscosity and relative viscosity, respectively, and c is the concentration of the polymer solution in units of g/ml.

The moisture absorption of the nylon 13,T sample was characterized using the method previously described by Kugel et al.[25] This method involved melt extrusion and compression of 3 g samples of nylon 13,T into small plaques using a Tinius Olsen MP600 Extrusion Plastometer. The analysis of moisture absorption was done using an Arizona Instruments Computrac 4000XL Moisture Analyzer. Sample plaques were soaked in distilled water for one week and adsorbed moisture was removed by towel drying the specimens prior to analysis. Samples were heated to 210 °C, while maintaining this temperature, mass loss was recorded. Once the mass loss slowed to 0.015% moisture/minute the analysis was complete and the total mass loss measured was recorded as the total moisture absorbed.

Results and Discussion

Chemical Characterization. Nylon 13,T was successfully synthesized using a two-step process. First, an aqueous solution of the TDA/TA monomer salt was held at 220 °C in a closed vessel for two hours before releasing the pressure to remove water vapor. This process produced a prepolymer/oligomer. The prepolymer was then transferred to a glass reactor equipped with a mechanical stir, oil bath, and vacuum line to produce high molecular weight polymer by melt condensation polymerization. The intrinsic viscosity of the polymer produced for the study was determined to be 0.62 dl/g.

The chemical composition of the polymer was confirmed using ^{1}H NMR, ^{13}C NMR, and FT-IR. Figures 1 and 2 display the ^{1}H NMR and FT-IR spectra, respectively. Peak area integration values and chemical shifts obtained from the ^{1}H NMR spectrum, shown in Figure 1, were consistent with the chemical structure of nylon 13,T. The FT-IR spectrum, shown in Figure 2, displayed characteristic peaks at 3303 cm^{-1} (N-H stretching), 1626 cm^{-1} (C=O stretching), and 1542 cm^{-1} (C-N stretching and CO-N-H bending) associated with the amide groups, peaks at 2921 cm^{-1} (CH_2 asymmetric stretching) and 2851 cm^{-1} (CH_2 symmetric stretching) associated with methylene groups derived from TDA, and a peak at 862 cm^{-1} (CH bending) associated with the aromatic ring derived from TA.[26]

Thermal Properties. The basic thermal properties of nylon 13,T were characterized using DSC. Figure 3 displays a DSC thermogram produced by heating a sample at 40 ^{o}C/minute. From this thermogram, a Tg at 90 ^{o}C and a melting transition with a peak centered at 263 ^{o}C is easily observed. The observed melting point is very similar to that reported for the commodity polyamide, nylon 6,6. Depending on the method of measurement and experimental conditions, the Tm of nylon 6,6 has been reported to be in the range of 260 to 270 ^{o}C.[25,27-29] While the Tm of nylon 13,T is similar to that of nylon 6,6, the Tg is significantly higher. The Tg of thoroughly dried nylon 6,6 has been reported to be in the range of 50 to 65 ^{o}C.[25,30,31] The higher

Tg of nylon 13,T can be attributed to the terephthalamide units in the polymer backbone that significantly decrease segmental mobility of the polymer backbone.

The melting transition as observed in Figure 3 displays two peaks. The first peak occurs at 221 °C and is followed by the major peak centered at 263 °C. The observation of two melting peaks may be due to a melting-recrystallization process as opposed to the presence of two different crystal structures. A common method for observing a melting-recrystallization process is to observe the melting transition using different heating rates during a DSC experiment. Figure 4 shows the melting transition observed using heating rates of 5, 20, and 40°C/minute. As shown in Figure 4, decreasing the heating rate reduces the prevalence of the lower temperature peak which is consistent with a melting-recrystallization process. By decreasing the heating rate, more time is available during the DSC experiment for the thinner crystallites, associated with the onset of melting, to melt and recrystallize into the thicker crystallites contributing to the main melting peak centered at 263 °C. The observation of multiple endothermic peaks in DSC thermograms resulting from a melting-recrystallization process has been observed with many polyamides including nylon 12,12,[32] nylon 12,14,[33] nylon 6,6,[34] and nylon 12,10.[35] It is interesting to note that, at the lowest heating rate (i.e. 5 °C/min.), a small endothermic peak centered at 273 °C was observed. This result suggest that this slow heating rate enables a fraction of the crystallites associated with the main melting transition centered at 263 °C to reorganize to form even thicker crystallites that melt at 273 °C.

The thermal stability of the nylon 13,T was characterized using TGA. Figure 5 displays TGA thermograms generating using both a nitrogen and air atmosphere. In general, the thermal stability of nylon 13,T is quite good with the onset of decomposition occurring around 300 °C and maximum decomposition rate occurring around 465 °C. By using the author's previously reported data,[25] a comparison between the thermal stability of nylon 6,6 and nylon 13,T can be made. For nylon 6,6, the temperature corresponding to 5 percent weight loss and 50 weight loss in a nitrogen atmosphere was determined to be 411 °C and 471 °C, respectively;[25] while that for nylon 13,T was 396 °C and 467 °C, respectively. Considering the Tm of nylon 13,T (Tm = 263 °C) and the thermal stability data, it can be expected that melting processing of nylon 13,T can achieved without extensive thermal degradation.

Crystallization Kinetics. The utility of a semicrystalline polymer for a given application and method of processing is highly dependent on the rate of crystallization. For example, nylon 6,6 is significantly faster crystallizing than nylon 6 which has resulted in nylon 6,6 being utilized to greater extent in applications involving processing by injection molding. For applications that utilize injection molding for the production of products, fast crystallization is desirable because it minimizes the "cooling time." The cooling time is the time required for sufficient crystallization to enable ejection of the molded product from the mold. In general, shorter cooling times translate to higher production rates of molded products. In contrast, for other methods of processing such as extrusion to produce fibers, filaments, film, and profiles, slower crystallization is desired to enable better control over shape and optical properties.[36] Thus, nylon 6 is often used for applications involving an extrusion process where slower crystallization is desirable. Crystallization rate also affects material properties such as modulus, impact strength, dimensional stability, and water absorption since these properties are dependent on the degree of crystallinity and crystalline morphology produced during processing. In general, modulus and dimensional stability increase with increasing crystallinity while impact strength and water absorption decrease with increasing crystallinity.

To understand the utility of nylon 13,T, a comparison of its crystallization rate to other commercially-relevant semicrystalline polymers was deemed useful. As discussed by Khanna,[37] a direct comparison of crystallization rates of different polymers can be difficult for multiple reasons. For example, the determination of isothermal crystallization kinetics using DSC is often limited to a very narrow temperature range since the crystallization process must be readily observed after reaching the crystallization temperature. If, at a given crystallization temperature, crystallization occurs very rapidly, the onset of crystallization may take place prior to reaching the isothermal crystallization temperature. In contrast, if crystallization occurs very slowly at a given crystallization temperature, the heat flow may be too subtle to be effectively observed. Thus, it may not be possible to compare the crystallization rate of different polymers at an equivalent degree of supercooling.

From a practical point-of-view, a comparison of Tm to the peak temperature of the crystallization exotherm (Tc) derived from controlled cooling from the melt can be useful for comparing the relative crystallization rate of different polymers. If an injection molding process is considered, it can be understood that a relatively small difference between Tm and Tc will result in a relatively high extent of crystallization because the onset of crystallization will be reached relatively quickly after injection of the molten polymer into the much colder mold. Using a heating and cooling rate of 20 °C/min, the value of Tm – Tc (ΔT) for the nylon 13,T sample was determined to be 22 °C. This value is considerably lower than the values previously determined by the authors[25] for nylon 6,6 ($\Delta T = 33$) and nylon 6 ($\Delta T = 46$). Thus, the crystallization rate of nylon 13,T is significantly higher than that of nylon 6,6 and nylon 6 suggesting potential utility for injection molding applications.

Khanna[37] proposed a parameter referred to as the crystallization rate coefficient (CRC) to directly compare the crystallization rates of different polymers. The CRC is determined using DSC and measuring Tc at three different cooling rates (i.e. 1.25, 10 and 40 °C/min). CRC is defined as the slope of the plot of cooling rate as a function of Tc. The basic premise behind the CRC is that the Tc measured for relatively fast crystallizing polymers will be less dependent on cooling rate than relatively slow crystallizing polymers. Khanna measured the CRC for seven different polymers including polyethylene terephthate (PET), poly(tetrafluoroethylene) (PTFE), nylon 6,6, and nylon 6. The values of CRC were consistent with expectations with PET possessing the lowest CRC (i.e. 38/hr), PTFE possessing the highest CRC (i.e. 153/hr), and nylon 6,6 possessing a higher CRC than nylon 6 (CRC for nylon 6,6 and nylon 6 was 82/hr and 54/hr, respectively). Using this method, the author's obtained a CRC for nylon 13,T of 164/hr, which is dramatically higher than that for either nylon 6,6 and nylon 6. The rapid crystallization observed for nylon 13,T coupled with the relatively high Tm and Tg suggests that this polymer would be

very useful as an engineering thermoplastic for injection molding applications. The rapid crystallization for nylon 13,T may be due to intermolecular interactions in the melt between the rigid terephthalamide units in the polymer chain that facilitate nucleation of crystallites upon cooling.

To obtain more detailed information regarding the crystallization process, isothermal crystallization kinetics were determined for nylon 13,T using DSC. Prior to measuring the isothermal crystallization kinetics, the equilibrium melting temperature (T°m) for nylon 13,T was determined using the Hoffman-Weeks approach, which involves the measurement of Tm as a function of isothermal crystallization temperature. According to the Hoffman-Weeks equation, shown below:

$$Tm = T°m(1 - 1/\gamma) + Tc/\gamma \qquad (II)$$

where Tm is the experimental melting temperature and γ is a factor that depends on the final lamellar thickness of crystallites, T°m can be determined by extrapolating the plot of Tm as a function Tc to the Tm = Tc line.[38] As shown in Figure 6, T°m was determined to be 289 °C. Based on this result, samples for measuring isothermal crystallization kinetics were heated above T°m to 300 °C to ensure complete melting of even the thickest crystallites.

The very rapid crystallization of nylon 13,T limited the range of crystallization temperatures that could be used for determining the isothermal crystallization kinetics. Figure 7 displays crystallization isotherms for crystallization temperatures ranging from 235 to 240 °C. From this data, the half-time of crystallization ($t_{1/2}$), defined as the time required to reach 50% of the total degree of crystallinity, can be obtained. Often, $t_{1/2}$ or $1/t_{1/2}$ is taken as a measure of the overall rate of crystallization. Figure 8 shows a plot of $t_{1/2}$ as a function of supercooling (i.e. ΔT = T°m – crystallization temperature). As expected, $t_{1/2}$ decreased with increasing ΔT since crystallization is nucleation controlled over this temperature range. The data from the crystallization exotherms can also be used to obtain information relevant to the mechanism of crystallization by determining the Avrami parameters, K and n, shown in the Avrami equation:

$$X(t) = 1 - \exp(-Kt^n) \qquad (III)$$

where X(t) is the relative extent of crystallization at time t, K is the crystallization rate parameter, and n is the Avrami exponent.[39,40] The Avrami exponent provides information about the crystal growth geometry and the nucleation mechanism. Since the Avrami equation was based on the assumption that the radial grow of crystals occurs at a constant velocity and, thus, impingement of crystals with one another does not occur, only data pertaining to relatively low extents of crystallization were used for the Avrami analysis. Figure 9 shows plots based on a rearranged version of the Avrami equation that enables n to be obtained from the slope of the lines and K to be obtained from the intercept. Table I lists values for the Avrami parameters. The Avrami exponent, n, was found to range between 1.5 and 2.0. According to theory, the values obtained for the Avrami exponent suggest heterogeneous nucleation and one dimensional crystal growth.[41] A heterogeneous nucleation mechanism is common for polymers since adventitious impurities, such as dust particles, that effectively nucleate crystallization are difficult to exclude from a sample.[42] One dimensional crystal growth for quiescent crystallization of a nylon is unusual. As discussed by Magill,[43] Avrami exponents ranging from 2 to 6 have been reported for polyamides. Assuming the Avrami exponent values obtained for nylon 13,T truly represent the mechanism of nucleation and growth and are not the result of violations of assumptions made in the derivation of the Avrami equation, such as a constant crystal growth rate, the relatively low Avrami exponents may be due to the existence of order in the melt. Avrami numbers below 2 obtained for isotactic polypropylene have been attributed to order in the polymer melt stemming from the helical structure of individual molecular chains.[44] Perhaps the relatively rigid terephthalamide segments of the chain form intermolecular interactions in the melt that exist beyond T°m and subsequently affect the crystallization process upon cooling. A complete understanding of the nucleation and crystal growth processes cannot be completely understood using just the Avrami analysis. Further characterization using, for example, optical microscopy is required to fully understand the mechanism of crystallization.

Since values of K were obtained at different crystallization temperatures, the activation energy (ΔE) associated with the crystallization rate parameter was determined using the Arrhenius relationship:

$$K^{1/n} = k_o \exp(-\Delta E/RT_c) \qquad (IV)$$

where k_o is the temperature-independent pre-exponential factor, R is the gas constant, and T_c is the crystallization temperature. By rearranging equation IV, ΔE can be obtained from the slope of a plot of (lnK)/n versus $1/T_c$ (Figure 10). For nylon 13,T, ΔE was determined to be 314.6 kJ/mol.

Crystal Structure. The crystal structure of nylon 13,T was characterized using WAXD. In general, the crystal structure of nylons can be divided into two main types referred to as the α and γ structures.[45] The α structure is common for even-even nylons such as nylon 6,6 and nylon 6,10. The polymer chains in the α structure are fully extended in the planar zig-zag conformation forming planar sheets of hydrogen bonds which are stacked upon one another. The crystal symmetry for even-even nylons with this structure is triclinic with one repeat unit per unit cell, while the crystal symmetry for even nylons such as nylon 6 is monoclinic with four repeat units per unit cell. The γ structure was originally defined by Kinoshita[46] and is commonly adopted by even nylons with more than seven carbons atoms as well as even-odd, odd-even, and odd-odd nylons. The unit cell of the γ structure when viewed in cross-section normal to the *c*-axis is comprised of extended chains that form the corners of a hexagon and is

termed a pseudohexagonal unit cell. For nylons possessing the α structure, two diffraction signals at a spacing of 0.44 and 0.37 nm are observed, while nylons exhibiting the γ structure show one strong reflection with a spacing of 0.42 nm.[47]

Figure 11 displays the WAXD pattern obtained for nylon 13,T. Two strong reflections corresponding to d-spacings of 0.42 nm and 2.3 nm were observed. The d-spacing of 0.42 nm is consistent with a pseudohexagonal unit cell. The 2.3 nm d-spacing corresponds to the dimension of the *c*-axis of the hexagonal unit cell. Compared to other long chain polyamides such as the odd-odd polyamides based on undecanedioic acid investigated by Cui and coworkers,[48] this d-spacing is considerable larger which can be attributed to the long thirteen carbon chain derived from TDA.

Moisture Absorption. The amide linkages of nylons serve as both hydrogen bond donors (through the amide NH) as well as hydrogen bond acceptors (through the amide carbonyl). The ability of the amide groups to donate and accept hydrogen bonds provides many of the desirable properties associated with nylon polymers such as relatively high thermal properties, abrasion resistance, and ductility. These desirable properties stem for intermolecular hydrogen bonds between amide groups. One the other hand, in a moist environment, these intermolecular hydrogen bonds can be displaced by hydrogen bonding interactions with water molecules that can greatly affect mechanical properties, thermal properties, and dimensional stability. In general, the higher the amide content, the higher the equilibrium moisture content at a given relative humidity. For example, at 23 ºC and 100 percent relative humidity, the equilibrium moisture content for nylon 4,6, nylon 6,6, nylon 6,10, and nylon 6,12 was reported to be 15, 8.5, 1.4, and 1.2 weight percent, respectively.[49]

Considering the exceptionally low amide content and fast crystallization of nylon 13,T, it was expected that the moisture uptake would be very low. The method used for characterizing moisture absorption of nylon 13T has also been previously used by the authors to measure moisture absorption for nylon 6,6 and nylon 6.[25] Values of moisture absorption for nylon 6, nylon 6,6, and nylon 13,T were 7.66 $\pm$ 0.07, 4.66 $\pm$ 0.14, and 0.27 $\pm$ 0.24 weight percent, respectively. As expected, the moisture absorption for nylon 13,T was exceptionally low for a polyamide which can be attributed to the low content of amide groups resulting from the long carbon chain length of TDA. This result suggests that the properties of nylon 13,T should be much less sensitive to moisture than most other nylons.

Conclusion

To the best of the author's knowledge, this document is the first description of the synthesis and characterization of nylon 13,T. Successful polymerization was accomplished using a two-step process involving oligomerization using a pressure vessel followed by high temperature melt condensation polymerization. Characterization of the thermal properties showed that nylon 13,T possesses a Tm similar to nylon 6,6 and a significantly higher Tg (i.e. 90 ºC), and very fast crystallization. In addition, the thermal stability was determined to be adequate enough to enable melt processing without significant thermal degradation. Due to the much lower amide content of nylon 13,T, water absorption was found to be dramatically lower than the industrially important nylons, nylon 6 and nylon 6,6. This result indicates that objects produced from nylon 13,T should have better dimensional stability in humid environments than objects derived from nylon 6 or nylon 6,6. Considering the data generated, nylon 13,T may have significant utility as an injection moldable engineering thermoplastic. Further work involving the characterization of mechanical properties is in progress.

Acknowledgement

The authors acknowledge the Department of Energy for financial support through grant DE-FG36-08GO88160.

Disclaimer

References

1. Xu, Y.; Hanna, M. A.; Isom, L. Green Chemicals from Renewable Agricultural Biomass: A Mini Review, *The Open Agriculture Journal*. **2008**, *2*, 54-61.
2. Dodds, D. R.; Gross, R. A. Chemicals from Biomass, *Science*. **2007**, *318*, 1250-1251.

3. Salimon, J.: Salih, N.; Yousif, E. Industrial development and applications of plant oils and their biobased oleochemicals, *Arabian J. Chem.* **2012**, *5*, 135-145.
4. Montero de Espinosa, L.; Meier, M. A. R. Plant oils: The perfect renewable resource for polymer science?!, *Eur. Polym. J.* **2011**, *47*, 837-852.
5. Baumann, H.; Buhler, M.; Fochem, H.; Hirsinger, F.; Zoebelein, H.; Falbe, J. Natural Fats and Oils – Renewable Raw Materials for the Chemical Industry, *Angew Chem, Int Ed Engl*. **1988**, *27***,** 41-62.
6. Meier, M. A. R.; Metzger, J. O.; Schubert, U. S. Plant oil renewable resources as green alternatives in polymer science, *Chem Soc Rev*. **2007**, *36*, 1788-1802.
7. Xia, Y.; Larock, R. C. Vegetable oil-based polymeric materials: synthesis, properties, and applications, *Green Chem.* **2010**, *12*, 1893-1909.
8. Mallegol, J.; Lemaire, J.; Gardette, J-L. Drier influence on the curing of linseed oil, *Prog Org Coat*. **2000**, *39*, 107-113.
9. Derksen, J. T. P.; Cuperus, F. P.; Kolster, P. Renewable resources in coatings technology: a review, *Prog Org Coat*. **1996**, *27*, 45-53.
10. Hill, K. Fats and oils as oleochemical raw materials, *Pure Appl Chem*. **2000**, *72*, 1255-1264.
11. Zuo, J.; Li, S.; Bouzidi, L.; Narine, S. S. Thermoplastic polyester amides derived from oleic acid, *Polymer*. **2011**, *52*, 4503-4516.
12. Perkins, R. B.; Roden, J. J.; Tanquary, A. C.; Wolff, I. A. Nylons from vegetable oils: - 13, -13/13, and -6/13, *Mod Plast*. **1969**, *46*, 136-142.
13. Vasishtha, A. K.; Trivedi, R. K.; Das, G. Sebacic acid and 2-octanol from castor Oil, *J Am oil Chem Soc*. **1990**, *67*, 333-337.
14. Azcan, N.; Demirel, E. Obtaining 2-octanol, 2-octanone, and sebacic acid from castor oil by microwave-induced alkali fusion, *Ind Eng Chem Res*. **2008**, *47*, 1774-1778.
15. Carlson, K. D.; Sohns, V. E.; Perkins, R. B.; Huffman; E. L. Brassylic acid: Chemical intermediate from high-erucic oils, *Ind Eng Chem, Prod Res Dev*. **1977**, *16*, 95-101.
16. Tomaszewski, W.; Wlochowicz, A.; Slusarczyk, C. Supermolecular structure of the nylon 6.10 crystallized from the melt and its changes during neating, *Applied Crystallography: proceedings of the XVI Conference*. **1995**, 274-277.
17. Koning, C.; Teuwen, L.; de Jong, R.; Janssen, G.; Coussens, B. Polyamides 4.10 and 4.12 and their isomers, *High Perform Polym*. **1999**, *11*, 387-394.
18. Franco, L.; Cooper, S. J.; Atkins, E. D. T.; Hill, M. J.; Jones, N. A. Nylon 69 can crystallize with hydrogen bonding in two and in three interchain directions, *J Polym Sci, Part B: Polym Phys*. **1998**, *36*, 1153-1165.
19. van Dyne, D. L.; Blasé, M. G. Process design, economic feasibility, and market potential for nylon 1313 produced from erucic acid, *Bioechnol Prog*. **1990**, *6*, 273-276.
20. Kawahara, S.; Matsuoka, H. Genestar heat-resistant polyamide. Responding to micromolding applications, *Purasuchikkusu Eji*. **2010**, *56*, 75-78.
21. Uddin, A. J.; Ohkoshi, Y.; Gotoh, Y.; Nagura, M.; Endo, R.; Hara, T. Melt spinning and laser-heated drawing of a new semiaromatic polyamide, PA9-T fiber, *J Polym Sci, Part B: Polym Phys*. **2004**, *42*, 433-444.
22. Measurement made by the authors using differential scanning calorimetry. The sample was Genestar® PA9T-N1000A M41.
23. Moreau, J. J. E.; Vellutini, L.; Wong Chi Man, M.; Bied, C.; Dieudonne, P.; Bantignies, J-L.; Sauvajol, J-L. Lamellar bridged silsequioxanes: Self-assembly through a combination of hydrogen bonding and hydrophobic interactions, *Chem Eur J*. **2005**, *11*, 1527-1537.
24. Solomon, O. F.; Ciuta, I. Z. Détermination de la viscosité intrinsèque de solutions de polymères par une simple détermination de la viscosité, *J Appl Polym Sci*. **1962**, *6*, 683-686.
25. Kugel, A.; He, J.; Samanta, S.; Bahr, J.; Lattimer, J.; Fuqua, MA.; Ulven, C.; Chisholm, B. J. Semicrystalline polyamide engineering thermoplastics based on the renewable monomer, 1,9-nonae diamine: thermal properties and water absorption, *Polym.-Plast Technol*. **2012**, *51*, 1266-1274.
26. Silverstein, R. M.; Bassler, G. C.; Morrill, T. C. *Spectrometric identification of organic compounds*, 4th ed. New York, NY: John Wiley & Sons, 1981.
27. Lee, S. S.; Phillips, P. J. Melt crystallized polyamide 6.6 and its copolymers, part I. Melting point – lamellar thickness relations in the hompolymer, *Eur Polym J*. **2007**, *43*, 1933-1951.
28. Pfluger, R. *Polymer Handbook*, 3rd Ed. Brandrup, J.; Immergut, E. H. Eds. New York, NY: John Wiley & Sons, 1989, pp. V/113.
29. Vouyiouka, S. N.; Papaspyrides, C. D. Catalyzed Solid-State Polyamidation, *Pfaendner R. Macromol Mater Eng*. **2006**, *291*, 1503-1512.
30. Qiu, W.; Habenschuss, A.; Wunderlich, B. The phase structure of nylon 6.6 as studied by temperature-moduluated calorimetry and their link to X-ray structure and molecular motion, *Polymer*. **2007**, *48*, 1641-1650.
31. Rios De Anda, A.; Fillot, L. A.; Rossi, S.; Long, D.; Sotta, P. Influence of the sorption of polar and non-polar solvents on the glass transition temperature of polyamide 6,6 amorphous phase, *Polym Eng Sci*. **2011**, *51*, 2129-2135.
32. Song, J. B.; Chen, Q. Y.; Ren, M. Q.; Sun, X. H.; Zhang, H. L.; Zhang, H. F.; Wang, S. Y.; Mo, Z. S. Multiple Melting and Crystallization Behavior of Nylon 1212, *Chin J Polym Sci*. **2006**, *24*, 187-193.
33. Li, Y.; Zhang, G.; Yan, D. Synthesis and crystallization behavior of nylon 12,14. I. Preparation and melting behavior, *J Appl Polym Sci*. **2003**, *88*, 1581-1589.

34. Magill, J. H.; Girolamo, M.; Keller, A. Crystallization and morphology of nylon-6,6 crystals: 1. Solution crystallization and solution annealing behavior, *Polymer*. **1981**, *22***,** 43-55.
35. Franco, L.; Puiggali, J. Structural data and thermal studies on nylon-12,10, *J Polym Sci Part B: Polym Phys*. **1995**, *33*, 2065-2073.
36. Roder, T. M.; Colbert, G. P.; Glenn, W. B.; Bongers, J.; Mooij, H. *Nylon Plastics Handbook, Kohan MI*. Ed. Cincinnati, OH: Hanser/Gardner Publications, 1995, pp 191-248.
37. Khanna, Y. P. A barometer of crystallization rates of polymeric materials, *Polym Eng Sci*. **1990**, *30*, 1615-1619.
38. Hoffman, J. D.; Weeks, J. J. Melting process and equilibrium melting temperature of poly(chlorotrifluoroethylene), *Res Natl Bur Stand US*. **1962**, *66A*, 13-28.
39. Avrami, M. Kinetics of phase change. I. General theory, *J Chem Phys*. **1939**, *7*, 1103-1113.
40. Avrami, M. Kinetics of phase change. II. Transformation-time relations for random distribution of nuclei, *J Chem Phys*. **1940**, *8*, 212-225.
41. Mandelkern, L. *Crystallization of Polymers*, New York, NY: McGraw-Hill, 1964, pp. 228.
42. Xenopoulos, A.; Clark, E. S. *Nylon Plastics Handbook, Kohan MI*. Ed. Cincinnati, OH: Hanser/Gardner Publications, 1995, pp. 121.
43. Magill, J. H. *Polymer Handbook*, Brandrup, J. Immergut , E. H. Eds. New York, NY: Wiley-Interscience, 1989.
44. Zhu, X.; Li, Y.; Yan, D.; Fang, Y. Crystallization behavior of partially melting isotactic polypropylene, *Polymer*. **2001**, *42*, 9217-9222.
45. Kinoshita, Y. The structures of polyamide series, *Makromol Chem*. **1959**, *33*, 1-20.
46. Kinoshita, Y. Crystal structure of poly(heptamethylene pimelamide) (nylon 77), *Makromo. Chem*. **1959**, *33*, 21-31.
47. Li, W.; Yan, D. Crystal Structure of Novel Polyamides with Long Diacid Segment: Polyamides 2 16, 4 16, 6 16, 8 16, 10 16, and 12 16, *Crysta Growth & Design*. **2003**, *3*, 531-534.
48. Cui, X.; Li, W.; Yan, D. Investigation of odd-odd nylons based on undecanedioic acid. 2: Crystal structures, *Polym Eng Sci*. **2005**, *45*, 1673-1679.
49. Williams, J. C. L.; *Nylon Plastics Handbook, Kohan MI* Ed. Cincinnati, OH: Hanser/Gardner Publications, 1995, pp. 324.

Table I. Kinetic parameters for nylon 13,T obtained from isothermal crystallization experiments.

Crystallization Temp. (°C)	Supercooling (°C)	$t_{1/2}$ (sec.)	K (sec.$^{-1}$)	n
235	54	19.8	7.68×10^{-2}	1.67
236	53	23.4	5.00×10^{-2}	1.56
238	51	28.2	4.85×10^{-2}	1.90
239	50	36.0	3.11×10^{-2}	1.95
240	49	43.8	2.19×10^{-2}	2.02

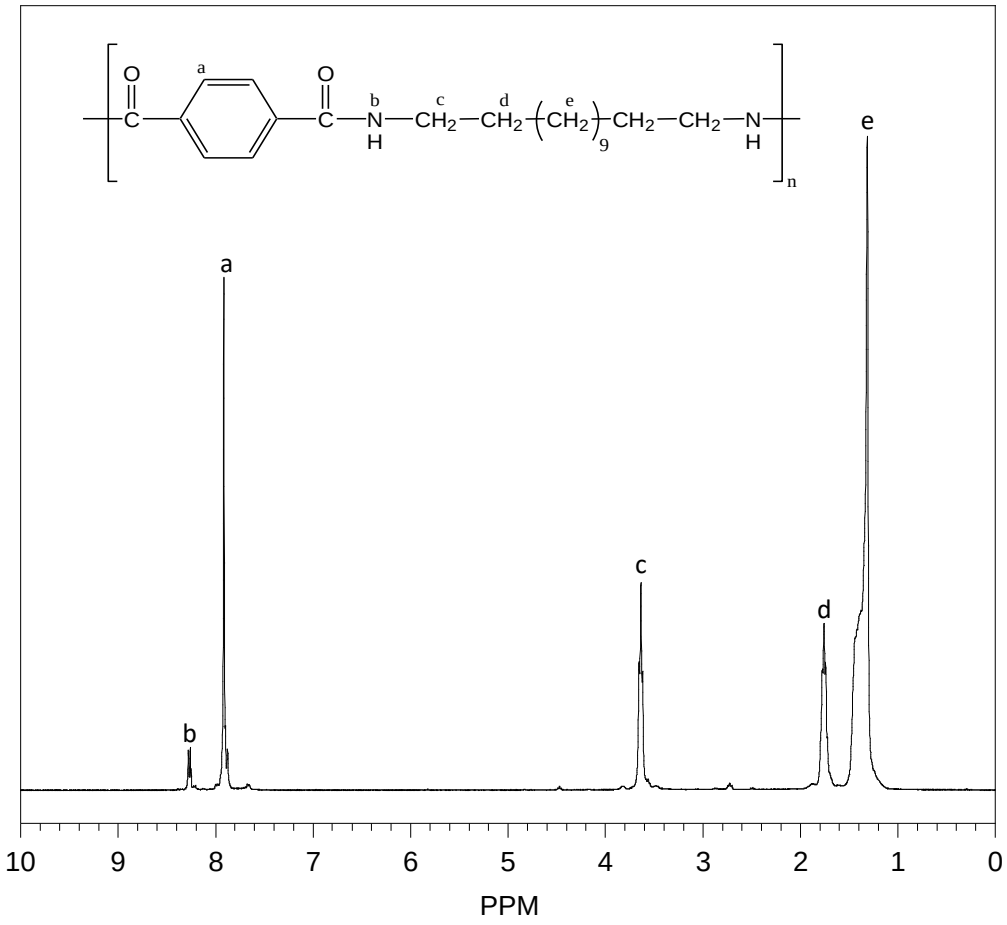

Figure 1. ^{1}H NMR spectrum of nylon 13,T.

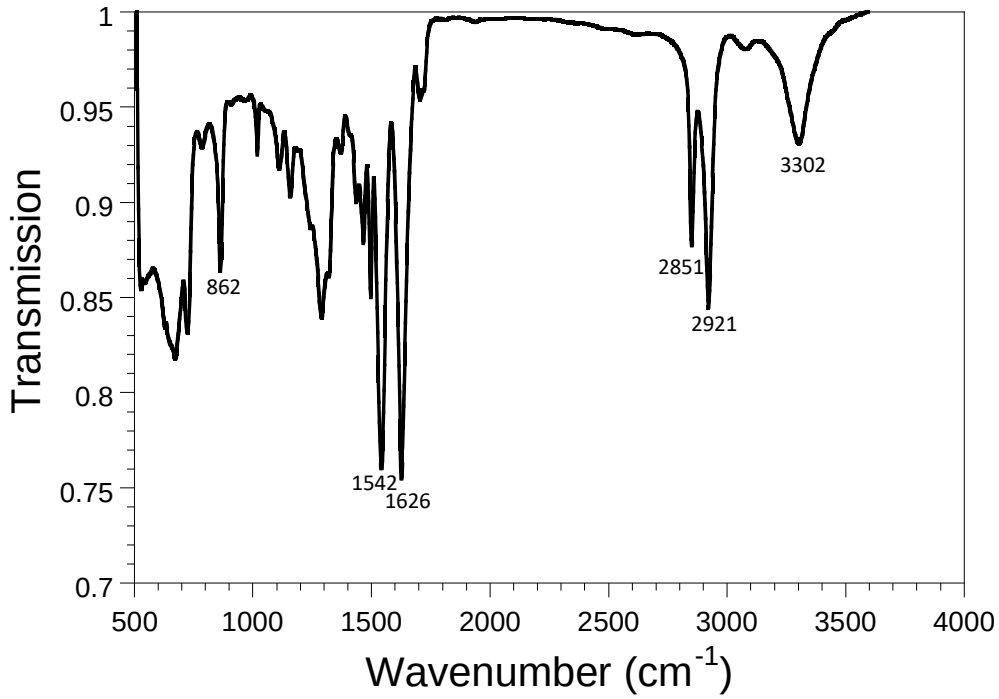

Figure 2. FT-IR spectrum of nylon 13,T.

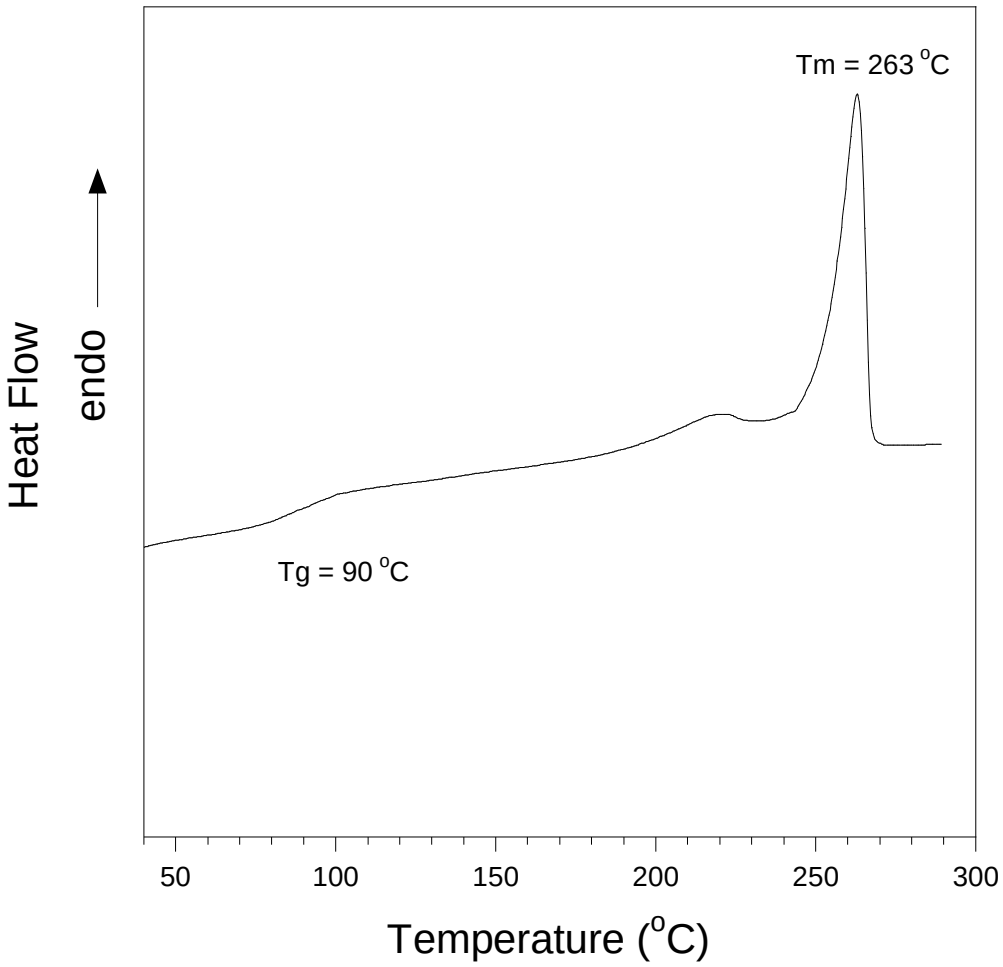

Figure 3. DSC thermogram of nylon 13,T generated by heating at 40 °C/min.

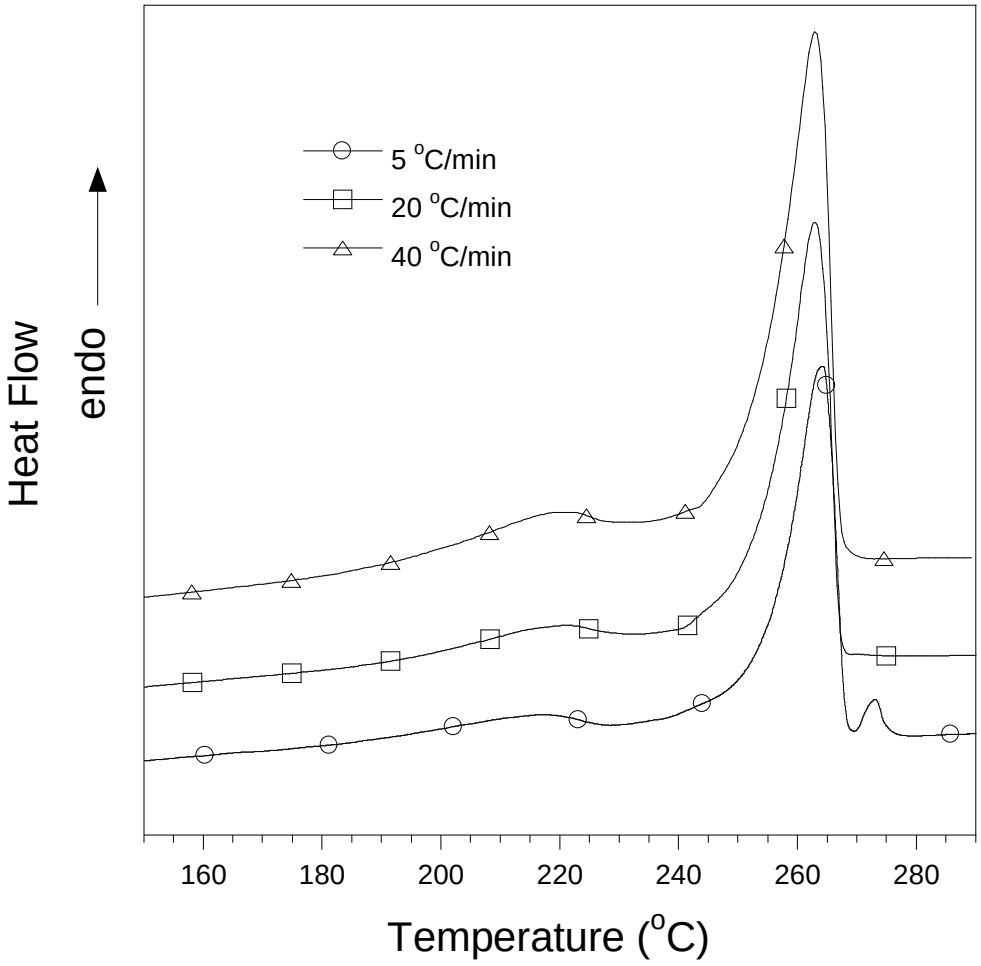

Figure 4. DSC thermograms of nylon 13,T produced using different heating rates.

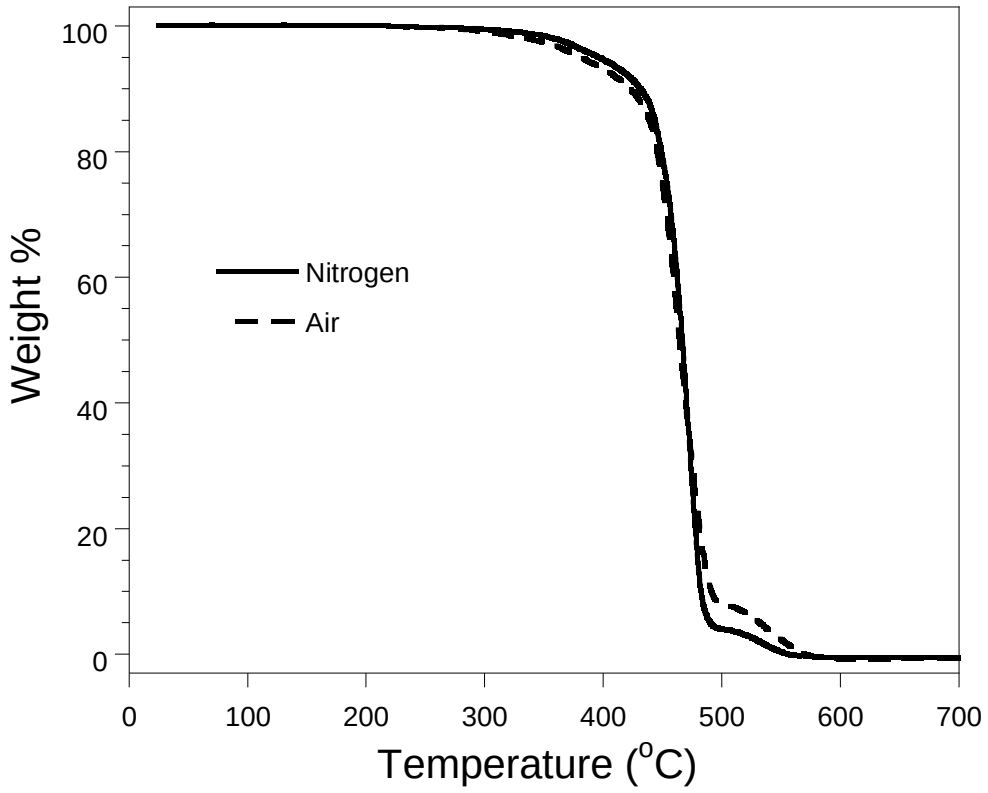

Figure 5. TGA thermograms produced using both an air and nitrogen environment.

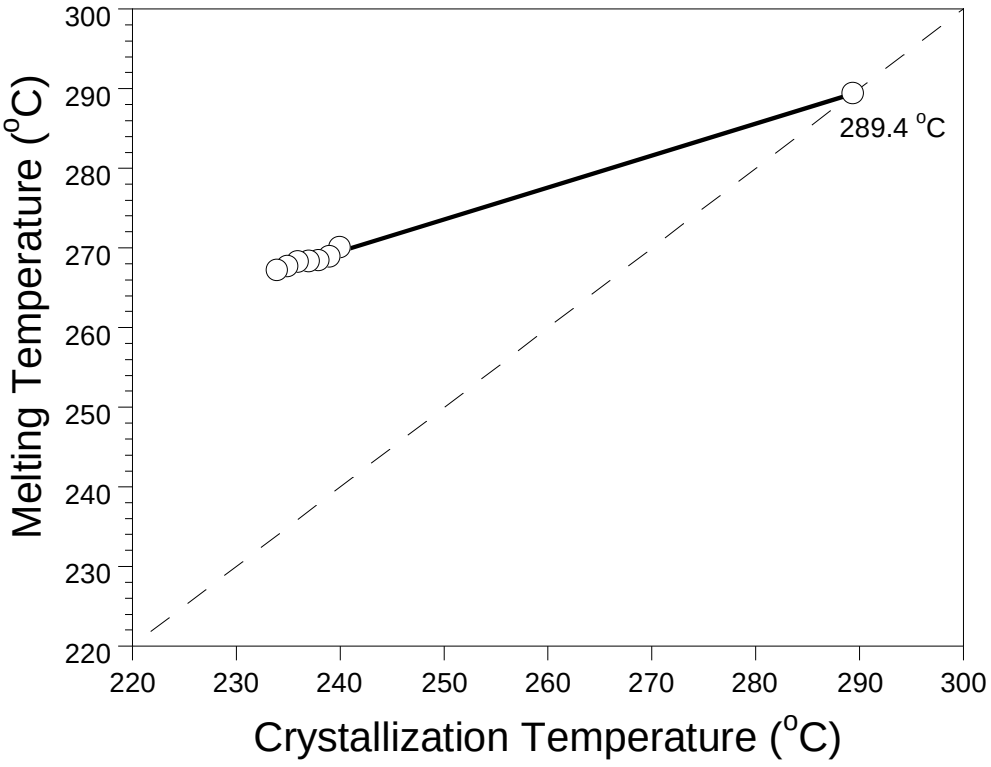

Figure 6. Plot of Tm as a function of isothermal crystallization temperature extrapolated to the Tm = crystallization temperature line. This plot enables the determination of the equilibrium melting temperature of nylon 13,T.

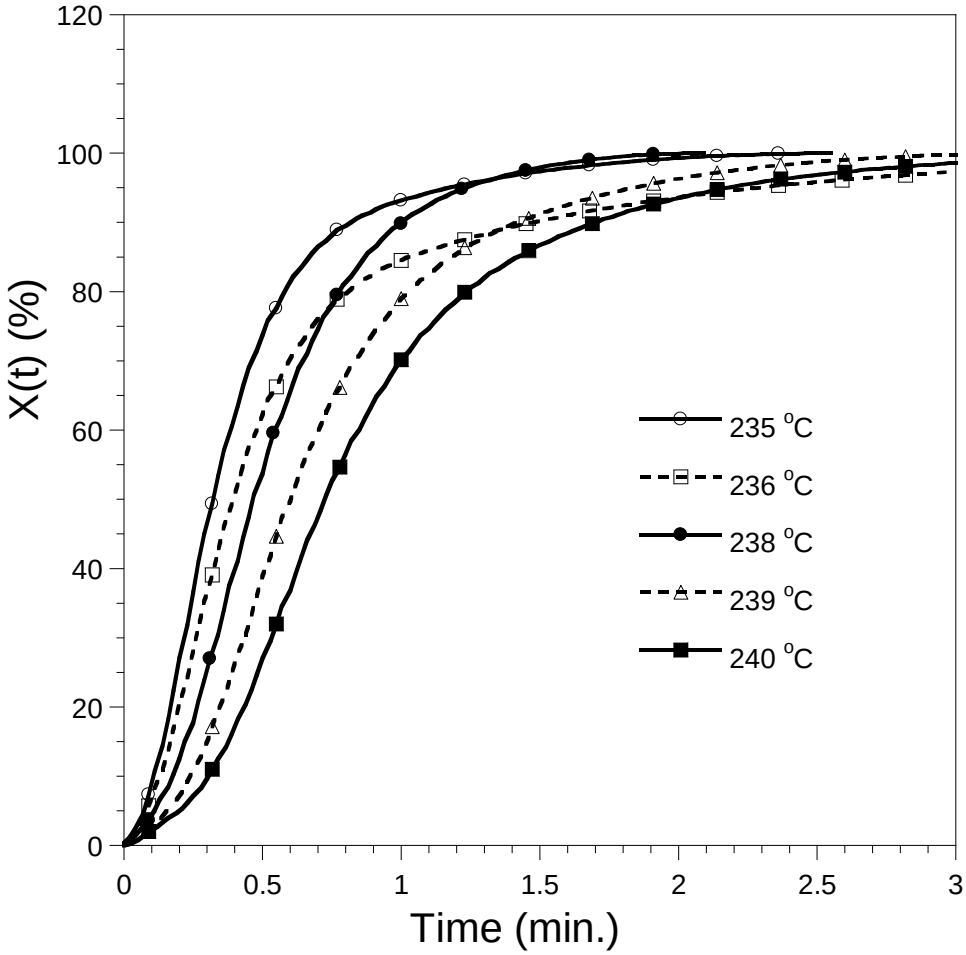

Figure 7. Crystallization isotherms obtained for nylon 13,T.

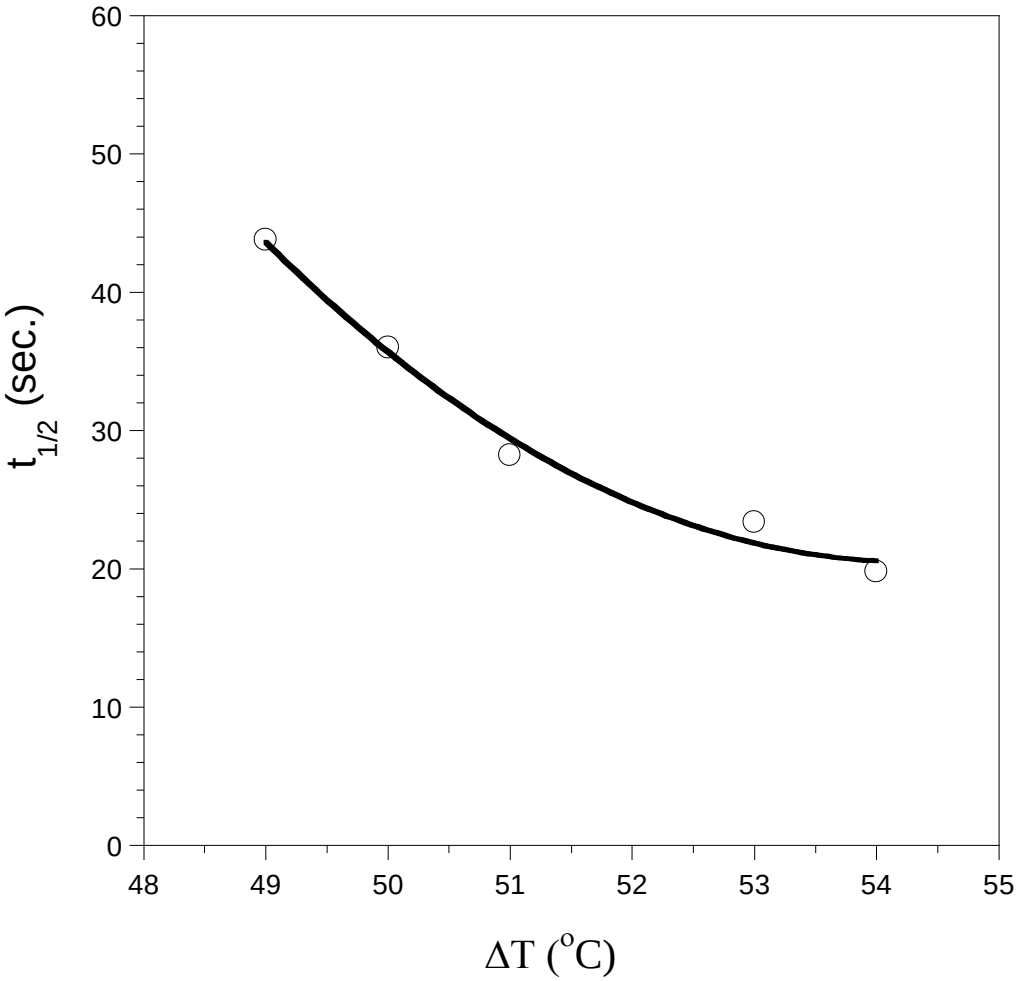

Figure 8. Plot of crystallization half-time ($t_{1/2}$) as a function of supercooling (i.e. ΔT = T°m – crystallization temperature) for nylon 13,T.

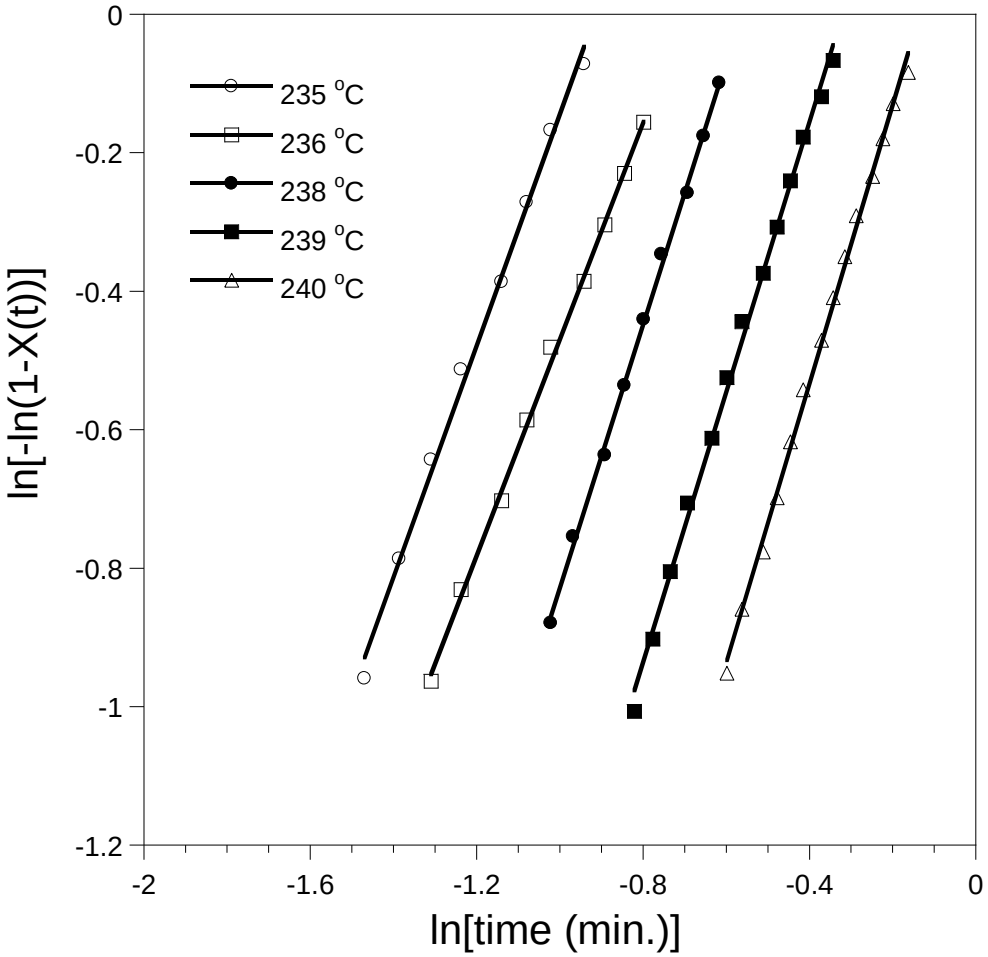

Figure 9. Plots based on the Avrami equation that enables n to be obtained from the slope of the lines and K to be obtained from the intercept.

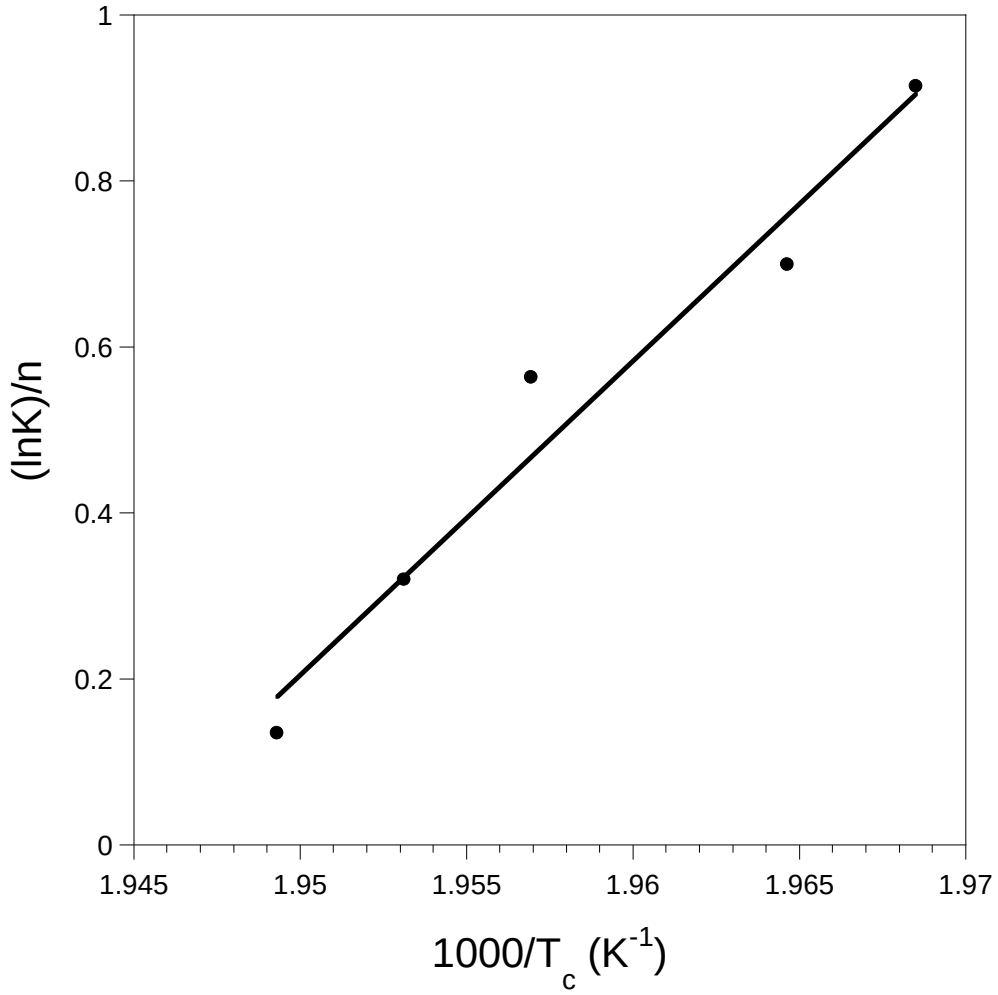

Figure 10. Plot based on the Arrhenius relationship that allows the activation energy associated with the Avrami crystallization rate parameter (K) to be determined from the slope of the line.

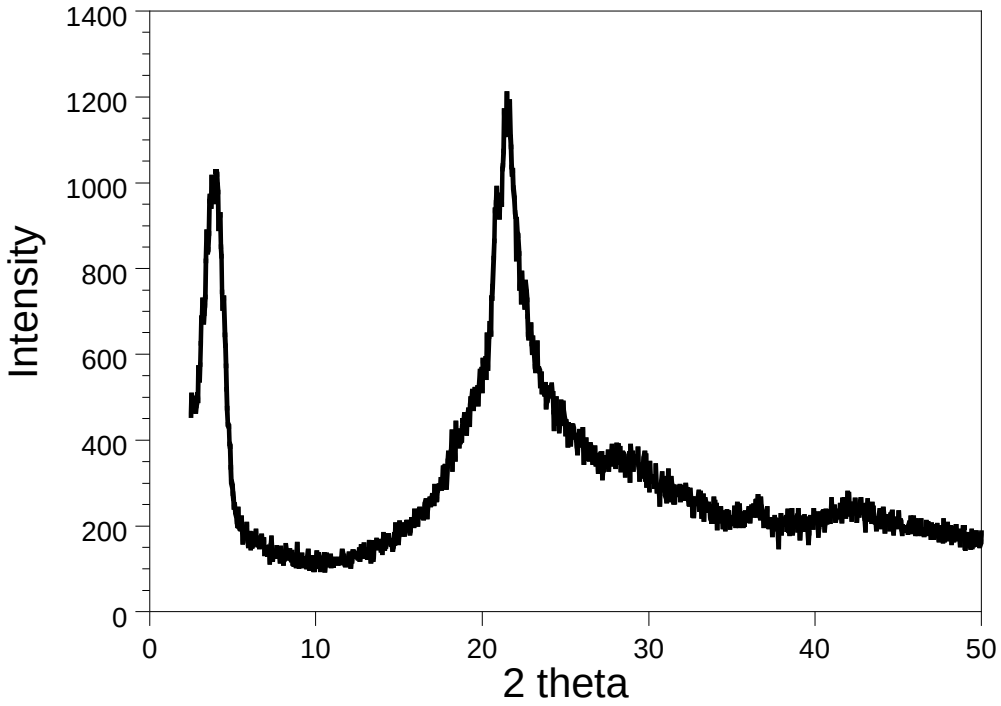

Figure 11. The WAXD pattern obtained for nylon 13,T.